NASA SP-5979 (01)
July 1975

TECHNOLOGY UTILIZATION

MATHEMATICAL TECHNIQUES

A COMPILATION

NATIONAL AERONAUTICS AND SPACE ADMINISTRATION

Foreword

The National Aeronautics and Space Administration has established a Technology Utilization Program for the dissemination of information on technological developments which have potential utility outside the aerospace community. By encouraging multiple application of the results of its research and development, NASA earns for the public an increased return on the investment in aerospace research and development programs.

Compilations are now published in one of nine broad subject groups:

SP–5971: Electronics – Components and Circuitry
SP–5972: Electronics Systems
SP–5973: Physical Sciences
SP–5974: Materials
SP–5975: Life Sciences
SP–5976: Mechanics
SP–5977: Machinery
SP–5978: Fabrication Technology
SP–5979: Mathematics and Information Sciences

When the subject matter of a particular Compilation is more narrowly defined, its title describes the subject matter more specifically. Successive Compilations in each broad category above are identified by an issue number in parentheses: e.g., the (03) in SP–5972(03).

This document is one in a series intended to furnish such technological information. Divided into three sections, this Compilation contains articles on theoretical and applied mathematics. Section 1 contains articles that might be of interest to workers in statistics and information theory. Section 2 includes descriptions of a number of computational aids that could be used by scientists and engineers; and Section 3 presents mathematical techniques for design and quality control.

Additional technical information on the items in this Compilation can be requested by circling the appropriate number on the Reader Service Card included in this Compilation.

The latest patent information available at the final preparation of this Compilation is presented on the page following the last article in the text. For those innovations on which NASA has decided not to apply for a patent, a Patent Statement is not included. Potential users of items described herein should consult the cognizant organization for updated patent information at that time.

We appreciate comment by readers and welcome hearing about the relevance and utility of the information in this Compilation.

Jeffrey T. Hamilton, *Director*
Technology Utilization Office
National Aeronautics and Space Administration

For sale by the National Technical Information Service, Springfield, Virginia 22161

Contents

Section 1. Statistics and Information Theory

THEORY AND CALCULUS OF CUBICAL COMPLEXES

Combination switching networks with multiple outputs may be represented by Boolean functions. A report has been prepared which describes the derivation and use of an extraction algorithm that may be adapted to the simplification of such simultaneous Boolean functions, a problem that often arises in logic minimization and fault diagnosis.

The algorithms are derived through cubical complexes, an n-variable, algebraic and topological system that may be used to represent a Boolean function of n-variables.

The particular problem that motivates the formulation of the extraction algorithm is a "covering" problem, i.e.: given a Boolean function, find an equivalent one in disjunctive form (the logical sum of logical products) that requires a minimum number of Boolean variables.

Each term of a Boolean function may be represented as:

$$X_1^{a_1} X_2^{a_2} \ldots X_n^{a_n}$$

where $X_i^{a_i} = X_1$ if $a_i = 1$, and $X_i^{a_i} = X_i'$ if $a_i = 0$

Each vertex of an n-cube (an n-dimensional hypercube) can be represented by the coordinates (a_1, a_2 ..., a_n) where $a_i = 0, 1$. Thus a one-to-one correspondence exists between the 2^n possible terms of the Boolean function and the 2^n vertices of an n-cube.

In developing the extraction algorithm, several concepts are defined. A 0-cube is a single vertex, a 1-cube consists of two zero cubes that differ in exactly one place (e.g., 1101 and 1100 which may be written as 110X where X is a free or "don't care" variable). A 2-cube would be of the form 11XX, and by induction the collection of r-cubes K^r is defined for all r where $0 \leq r \leq n$.

A cubical complex is defined as K^0, K^1, ... K^n and two operators, the face and co-face operators. Several other operations (a star product, a sharp product, and a "less than" operation) are defined for us in the extraction algorithm.

Several types of subcomplexes are defined and, along with the various operations, are used in an extraction algorithm to find a K-cover of minimum cost for a subset of K. This procedure, then, is analogous to finding the minimum number of literals and (logical) product terms necessary to represent a Boolean function in disjunctive form.

Source: Marvin Perlman of
Caltech/JPL
under contract to
NASA Pasadena Office
(NPO-11491)

Circle 1 on Reader Service Card.

BINARY CONCATENATED CODING SYSTEM

In many instances, data encoding by either delta (differential) modulation or a fully encoded scale is relatively inefficient. To understand the approach incorporated in each, consider a measurement application which uses a 1-meter rod divided into 1-centimeter intervals. If a given length were measured and processed by nonambiguous encoding, the readout would be a numerical value of the measured length in centimeters; that is each centimeter would be numbered. Delta modulation, on the other hand, measures unit intervals so that centimeters are not numbered. The user would, therefore, have to count centimeter lines to obtain the numerical value of a measurement.

A binary concatenated coding (BCC) system simplifies many types of measurements by using 3-bit binary words to count numbers from 0 through 99.

The system utilizes a decade type measurement scale which is divided into specific intervals. In each decade, integers 1 through 7 are described by 3-bit data words expressed in the binary system as 001 through 111, respectively.

The number 8, normally expressed in binary as a four-digit 1000, is depicted as 000. Numbers 9 and 10 are coded depending on the decade by binary 2, 3, or 4 for 9 and 4, 5, 6, or 7 for 10. Thus, 9 described in binary 2 and 10 described in binary 4 would indicate the second decade, etc. This would correspond, for example, to the 10th centimeter on the meter scale.

In use, this coding is applicable to any measurement which has an integer scale up to 100. The user who records a measurement through this coding obtains a decimal number from 1 through 10 as a 3-bit data word. This word is the last digit of the recorded value. To establish the decade (first digit) in which this reading is taken, he has to scan to the left on the readout and check the coding of the first 9's and 10's that he encounters. From this he can deduce the exact measurement value. This technique is highly competitive with pulse code and delta modulation for slowly varying measurements where continuous data readout is desirable.

This system which uses 6-bit data words can be expanded to read from 1 to 10,000, and 9-bit data words can increase the range to 1,000,000. In addition, the code may be "read" directly by observation after memorizing a simple listing of 9's and 10's.

Source: L. G. Monford, Jr.
Johnson Space Center
(MSC-14082)

Circle 2 on Reader Service Card.

ESTIMATING TIME TO RESTORE SERVICE IN A MULTICOMPONENT SYSTEM

This numerical technique reduces the complex statistical data describing a multicomponent system. It is used to obtain the expected value of an ordered statistic germane to a mixture of multiple-exponential distributions.

Specifically the technique is used to analyze systems in which if just one part fails, the whole system fails; and it is used to determine the "time to restore" service in such a case. An example is the range support equipment at a missile test facility.

The statistical technique evaluates the time required to repair components of different types and, thus, the time to have the whole system working by using the distribution of the nth-order statistic in a random mixed sample.

Source: H. I. Patel of
University of Georgia
under contract to
Marshall Space Flight Center
(MFS-20617)

Circle 3 on Reader Service Card.

VALIDITY TEST FOR LINEAR ERROR ANALYSIS

In linear, nonsequential, error analysis, batched data are used to obtain estimates which have the minimum error consistent with the completeness and accuracy of the data. This method is frequently compared to the more lengthy Monte Carlo technique. Under certain circumstances the two techniques are equivalent with the most important factor for equivalence being convergence. To determine whether the estimation process simulated by linear error analysis will converge, a new criterion, based on an extension of classical observability, has been developed. The particular application of this technique is with groups of batched navigation data where the statistics of the estimation errors are derived with classical minimum-variance methods.

The extended observability describes the extent to which the navigation is estimating the real world. The error ellipsoids are described by an asphericity factor. This factor measures the extent to which the shape of the ellipsoid is distorted from a spherical configuration. The extent to which the true error ellipse is represented by the estimated error ellipsoid is related to the observability. For instance, if the major axes of the ellipses are colinear, the overlap and thus the observability will be excellent; if the major axes are at right angles, the observability will be poor and the possibility of an error in the estimate will be greater.

Since alinement of the axes provides the most favorable observability, it can serve as the basis of the observability criterion. From the normalized asphericity factors, orientation of the axes may be obtained through a "sphericity transformation". From the transformation matrix a single, normalized "observability parameter" can be defined. This parameter has a value of 1 for maximum observability, 0 for neutral observability, and is negative for degraded observability.

If degraded observability is indicated, a failure likelihood test must be applied. The probability that error may arise depends on the distribution of the real and estimated errors, and may be calculated by a method using the orientation of the ellipses and existing techniques.

Source: L. S. Diamant of
TRW, Inc.
under contract to
Johnson Space Center
(MSC-14378)

Circle 4 on Reader Service Card.

A GENERALIZATION OF THE WEIBULL DISTRIBUTION

The two-parameter Weibull distribution (with origin at zero) and the three-parameter version (with origin at γ) are widely employed as statistical models in connection with life testing.

A new four-parameter generalization of this distribution provides a more versatile model, for life studies and related investigations. The technique develops analytical estimators of parameters, using maximum-likelihood estimators, moment estimators, and alternate estimators based on the first three moments and the first-order statistic.

This technique can be used to analyze the behavioral characteristics of complex operating systems, and in quality-control and product-testing applications for the electronics and automotive industries.

Source: A. C. Cohen of
University of Georgia
under contract to
Marshall Space Flight Center
(MFS-20612)

Circle 5 on Reader Service Card.

A METHOD FOR EXPANDING MULTINOMIALS FOR ANY NUMBER OF VARIABLES

A method has been developed for expanding multinomials to any order for any number of variables. The system can be easily implemented on a computer. Multinomials can be expanded using the binomial theorem or the multinomial theorem. A binomial expansion results in a very cumbersome equation, containing many summations. The multinomial expansion is a more manageable expression, but there is no provision for selecting the R numbers in the multinomial expansion formula:

$$(X_1+X_2+\ldots X_R)=\Sigma N!\prod_{i=1}^{R}\frac{X_i^{A_i}}{A_i!}$$

where the sum is taken of R numbers from 0 to N, such that

$$N=\sum_{i=1}^{R} A_i$$

An alternate way of choosing values for

$$\left\{A_i\right\}_{i=1}^{R}$$

is to construct all methods for putting N objects into R boxes, where A_i is the number of elements in the ith box. Thus the problem is solved by a program which will expand multinomials for any number of variables by using a set of recursive formulas that will generate all possible choices of

$$\left\{A_i\right\}_{i=1}^{R}$$

Source: G. M. Engel of
IBM Space Systems Center
under contract to
Marshall Space Flight Center
(MFS-91750)

Circle 6 on Reader Service Card.

SIMPLIFIED METHOD FOR FINDING ESTIMATORS IN CURTAILED ATTRIBUTE SAMPLING

A simplified method has been developed for delivering the maximum-likelihood estimation (MLE) of the fraction defectives, and of the average sample number (ASN), in single curtailed sampling. Obtaining estimators can be simplified, by choosing the number of items inspected as the basic random variable rather than an artificial variable.

The MLE (p), based on inspections from a sequence of m lots, is the ratio of the number of defectives found to the total number of items inspected. The symptotic variance of this estimator is approximately

$$\frac{\hat{p}(1-\hat{p})}{\sum_{i=1}^{m} Y_i}$$

where $\sum_{i=1}^{m} Y_i$ is the total of all items inspected.

The estimator is used for fraction detection in lot-attribute sampling plans, where sampling is discontinued when the lot is either accepted or rejected based on a specified number of defectives.

Source: A. C. Cohen of
The University of Georgia
under contract to
Marshall Space Flight Center
(MFS-20363)

Circle 7 on Reader Service Card.

INFORMATION RETRIEVAL FOR NONSTATIONARY DATA RECORDS

Most random time series recorded in a natural (uncontrolled) environment, such as the atmosphere, are affected continuously by the variations of the environment. These time series are statistically nonstationary. A compendium of the present techniques provides a working approach to the problems of analyzing nonstationary random data in determining trends, periodic components, and stationary random time series.

Three types of approach are given, the first being the classical theory of stationary time series. Statistical quantities such as mean, correlation, and spectrum are defined much the same as for stationary time series, except that an additional time or frequency parameter is introduced.

The second approach follows the model-construction method by assuming that the nonstationary time series consists of a slowly-varying trend, a periodic component, and a stationary random component. The basic strategy of this approach is to split the nonstationary time series into its components and then to analyze each component separately. In the third approach, which is a further refinement of the first approach, an optimum filtering operation is derived and performed on the double-parameter correlation, or spectrum function, obtained from the ensemble average.

A new algorithm for splitting nonstationary time series is presented as applied to the analysis of sunspot data.

Source: M. Y. Su of
Northrop Corp.
under contract to
Marshall Space Flight Center
(MFS-21929)

Circle 8 on Reader Service Card.

USING BAYESIAN STATISTICS TO ASSESS RATE-OF-COMPONENT FAILURE

Bayesian Statistics are used for early assessment of component failure rates. The classical method, T/n (where T is the component time and n is the number of failures), is often useless for the assessment, until a large quantity of data is available for the component in question. The Bayesian approach offers a better method, since it determines failure rate with limited test data.

Given a prediction which is reliable to the extent that $\bar{m}/2<m<2\bar{m}$ with reasonable certainty, where m is the predicted component MTBF (mean time between failure), a reasonable assumption of Bayes' estimate of m (the true component MTBF) is

$$\hat{m} = \frac{\bar{m}+T/4}{1+n/4}$$

where m is the assessed component MTBF.

The method allows the determination of equipment reliability tests for both commercial and military specifications, in pyrotechnics, navigation, ASW detection, appliances, and automotive parts, for example. Considerable cost savings result, since it is cheaper to correct potential failures than to incur the expenses of a system breakdown.

Source: R. M. Sireath, Jr., of
The Boeing Company
under contract to
Marshall Space Flight Center
(MFS-14749)

Circle 9 on Reader Service Card.

SENSITIVITY COEFFICIENTS GENERATED FOR USE IN DESIGNING MATHEMATICAL MODELS

Methods have been developed for the generation of first- and second-order sensitivity coefficients. The input/output relationship of the coefficients must be describable by a linear, ordinary, constant-coefficient differential equation of the following type:

$$a_n \frac{d^n c}{dt^n} + a_{n-1} \frac{d^{n-1} c}{dt^{n-1}} + \ldots + a_1 \frac{dc}{dt} + a_0 c =$$

$$b_n \frac{d^n r}{dt^n} + b_{n-1} \frac{d^{n-1} r}{dt^{n-1}} + \ldots + b_1 \frac{dr}{dt} + b_0 r$$

The coefficients of the equations may be functions of the system parameters, and the order of the numerator dynamics may be as great as the order of the denominator dynamics. It is shown that the first-order sensitivity coefficients with respect to each parameter, pj, j=1, 2, . . . , k, may be generated as linear combinations of the signals present in the system and one sensitivity model. The generation of the second-order sensitivity coefficients with respect to each parameter pj may be accomplished with k+1 sensitivity models in addition to the system model.

The first- and second-order output sensitivities may be used for the purpose of generating the first- and second-order sensitivities of a class of cost functionals. The cost sensitivities in turn are utilized for the purpose of determining parameter sets which yield a relative minimum in the cost functional.

An s-domain proof (Laplace transform) of the often-noted symmetry and complete simultaneity property of the first-order state sensitivities of a system in the companion canonical form is given. This proof is extended to the second-order state sensitivities.

As a result, the second-order state sensitivities with respect to any given number of system parameters may be generated utilizing two sensitivity models instead of k+1. Furthermore, the system need not be in the form of the equation. Removal of this restriction means that one does not need the transfer function between input and output. The system may be simulated in any form desired.

Source: C. L. Phillips of
Auburn University
under contract to
Marshall Space Flight Center
(MFS-21110)

Circle 10 on Reader Service Card.

PROBABILITY DENSITY FUNCTIONS IN COMPUTER DESIGN

Mathematical techniques based on probability models and the algebraic manipulation of probability density functions are necessary tools in designing complex information-processing systems. A procedure, superior to approximate methods and recommended for computer implementation, was developed at the Marshall Space Flight Center for work on a general-purpose spaceborne digital computer.

Two basic problems are considered:

1. Let p(x) be the probability density function of a random variable x; and y(x) an analytic, uniquely valued, and otherwise arbitrary function of x. Find the probability density function of y.

   The problem may be solved by a transformation rule:

$$p(y)dy = \sum_{i=1,(1),k} p\left(x^{(i)}\right) \left| \left(\frac{dx}{dy}\right)_{x=x^i} \right| dy$$

2. Let $p_k(x_k)$, k = 1, (1), n be the probability density functions of a set of random variables, x, k = 1, (1), n; and let $z = \phi(x_1, x_2, \ldots x_k)$, where z is an analytic, uniquely valued, and otherwise arbitrary function of $(x_1, x_2, \ldots x_k)$. Find the probability density function of z.

   The problem may be solved by a composition rule:

$$p(z) = \int_R \frac{\prod p_k(x_k)\, dx_k}{\left| \frac{\delta\phi}{\delta x_j} \right| dx_j}$$

where the product is taken over all n values of k and j is an arbitrary index between 1 and n. The integration manifold R is defined by $R = S \cap C$, where C is the manifold defined by $\phi(x) = z$ = constant and S is an n-dimensional manifold of certain points of x.

Proofs, examples, and several applications of these two methods are discussed. The technique is particularly applicable to computer design and error analysis.

Source: B. G. Grunebaum of
Computer Sciences Corp.
under contract to
Marshall Space Flight Center
(MFS-20611)

Circle 11 on Reader Service Card.

Section 2. Algorithms and Computational Aids

BINARY, OCTAL, AND HEXADECIMAL CONVERTER

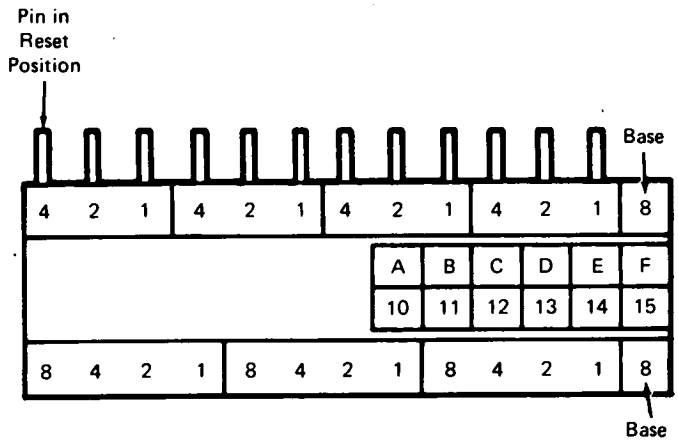

Number-System Converter

A simple mechanical device has been developed for the interconversion of numbers in the binary, octal, and hexadecimal number systems. This converter (see figure) consists of a block with 12 pins or keys. The positions of the keys are labeled with several scales, each of which is associated with a particular number system.

Numbers are converted from one system to another by pressing down a combination of pins. The conversion then may be read from the value of the positions indicated on the appropriate scale.

The converter is based on the binary number system, and each pin represents the set/reset states of a binary bit; i.e., set or "1" when the pin is pressed down, and reset or "0" when it is up. The positions of the pins give a direct readout of the binary number at the top of the scale.

Programers, who often need to transform binary information into another number system, will find this converter especially useful. It can be manufactured inexpensively from plastic by a conventional molding process.

Source: J. M. Lee of
Philco-Ford Corp.
under contract to
Johnson Space Center
(MSC-12595)

Circle 12 on Reader Service Card.

CURVE FITTING TO REDUCE CALCULATION TASK

Tests and experiments often yield data points for which two parameters vary nonlinearly with a third parameter that cannot be directly measured. No standard technique exists for relating three such parameters mathematically, as would be needed if they were used for a computer calculation.

The previous method has been to graph the relationships between the nonmeasurable parameter and one other, and to then read off data points which are fed into a computer in tabular form. The computer then calculated the values of the nonmeasurable parameter for the given values of the other two. Because of the nonlinear characteristic of the data graph and the usual wide separation between data points, accuracy has been very limited with this technique.

Instead, the nonmeasurable empirical parameter can be expressed as a continuous function of the two measurable empirical parameters. The continuity means that linear interpolation no longer need be used to determine dependent variables of nonlinear functions.

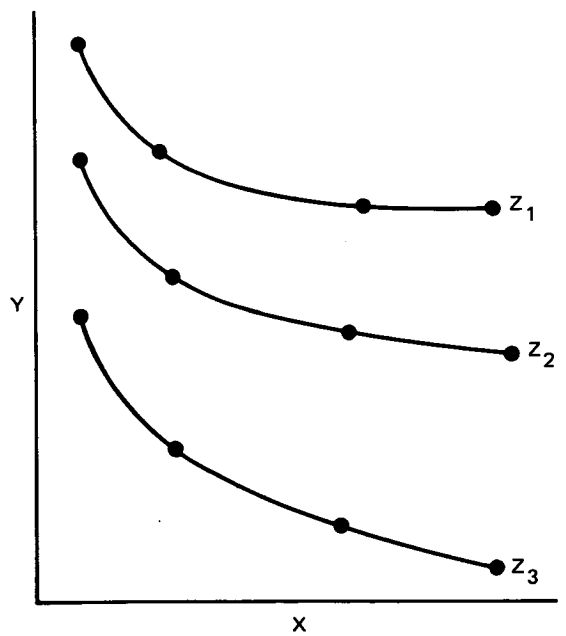

Three-Variable Functions Y = f (X, Z)

The relationship may be understood by referring to the figure. A least-squares expression is derived between X and Y for each value of Z:

$$\text{E.g., for } Z_1\text{: } Y = A_{01}+A_{11}X+A_{21}X^2 \ldots +A_{n1}X^n$$

$$\text{for } Z_2\text{: } Y = A_{02}+A_{12}X+A_{22}X^2 \ldots +A_{n2}X^n$$

As Z varies, the values of the coefficients vary, usually as a smooth function of Z. Each coefficient may therefore be expressed as a function of Z, which may be obtained by another least-squares fit:

$$\text{E.g., } A_0 = B_{00}+B_{01}Z+B_{02}Z^2 \ldots +B_{0m}Z^m$$

$$A_1 = B_{10}+B_{11}Z+B_{12}Z^2 \ldots +B_{1m}Z^m$$

These are then combined to produce an expression relating all three parameters:

$$Y = (B_{00}+B_{01}Z \ldots B_{0m}Z^m)+(B_{10}+B_{11}Z \ldots +B_{1m}Z^m)X+ \ldots +(B_{n0}+B_{nl}Z \ldots +B_{nm}Z^m)X^n$$

When working with data that follow logarithmic curves, individual curves may be fitted as A_{ij}ln X. Likewise the equations for the A_{ij} may be reset in logarithmic form when that procedure results in a more accurate fit.

This method can be particularly helpful where limited-capacity computers are used, such as with automatic quality-control systems or programable calculators. In addition, the technique is not limited to empirical data. For instance, tables used as input data (such as temperature and pressure tables for thermodynamic calculations) could be stored in equation form rather than as tables.

Source: D. R. Saucier, Jr.
Johnson Space Center
(MSC-13406)

No further documentation is available.

A METHOD FOR RAPIDLY EVALUATING THE LINEARITY OF CALIBRATION DATA

A simple technique is presented for determining whether or not a set of five data points lies within a specified close tolerance of a linear fit.

The following theorem, which justifies this technique, will be proved: Define two arbitrary constants, T and C. Select data points (X_i, Y_i) with i = 1,2,3,4,5 which have the property

$$X_{i+1} - X_i = C. \quad (1)$$

Let $f(X) = a_0 + a_1 X$ be the least-squares linear fit to these data (regression of Y on X). If $g(X) = b_0 + b_1 X$ is another line which has the property

$$Y_i - g(X_i) < T/1.6 \text{ for all i}, \quad (2)$$

then $$Y_i - f(X_i) < T \text{ for all i}. \quad (3)$$

Consider the following situation. A calibration check is run on amplifier modules with a linearity tolerance of 0.25% of the full-scale output. The input signal is increased in five equal steps. Full scale output is approximately 5 V (tolerance 0.0125 V). The expected results follow:

Coded Input	Nominal Output
0	0.00 V
1	1.25 V
2	2.50 V
3	3.75 V
4	5.00 V

A logical first step to verify acceptable data linearity is to plot the points and see if a line can be drawn to bring the points within tolerance. In this case, however, if a graph is plotted using a scale of 1 V: 2 in., the tolerance is only 0.025 in., less than 1/32 in. Thus, plotted on 8-1/2 x 11 in. graph paper, the tolerance in question is barely discernible. To avoid this problem of scale, a difference plot is used.

Full-Scale Graph of Data Points and Reference Line

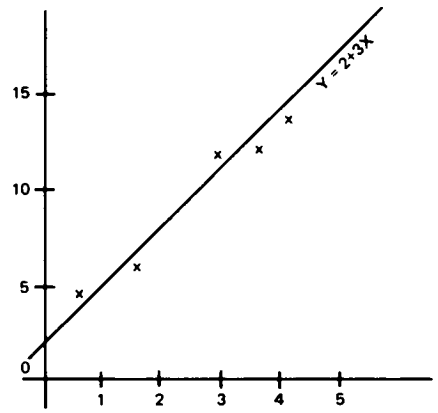

X_i	Y_i	Difference Between Y_i and Corresponding Point on Line
1	6	+1
2	7	−1
3	12	+1
4	12	−2
5	16	−1

Figure 1. Sample Data Set

Difference Plot and Least-Squares Straight-Line Fit

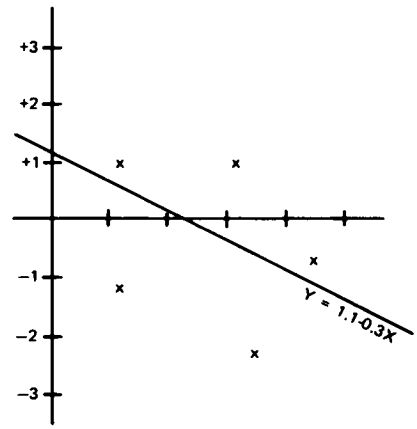

X	Difference	Fitted Difference By Method of Least-Squares	Residual
1	+1	0.6	0.4
2	−1	0.1	−1.1
3	+1	−0.4	1.4
4	−2	−0.9	−1.1
5	−1	−0.4	0.4

Figure 2. Difference Plot

Figure 1 presents a sample data set (chosen deliberately to exaggerate certain aspects of difference plots) in tabular and graphic form, together with an approximately fit reference line: Y = 2+3X. Figure 2 shows the difference plot, a graph of the vertical separation of each point from the reference line. These differences may be plotted on a magnified scale, to allow easy display of discrepancies otherwise too small to see. The line plotted on Figure 2 is the least-squares best fit to the difference data

$$h(X) = 1.1 - 0.3X \tag{4}$$

In general, the least-squares line h(X) fitted to a difference plot is related to the reference line g(X) used to determine the differences and to the least-squares line f(X) fitted to the raw data, by the relationship

$$f(X) = g(X)+h(X). \tag{5}$$

Thus, in this example, f(X) may be computed from the sum

$$\begin{aligned} g(X) &= 2.0+3.0X \\ h(X) &= 1.1-0.3X \\ f(X) &= 3.1+2.7X \end{aligned}$$

Worst-case analysis was used to obtain the constant 1.6 which appears in equation 2. Let the tolerance on the y-distance be unity. Then the worst case of a line within tolerance exists when each of the five points is at the maximum distance of ±1 from the reference line. There are 32 such cases, but, because of the condition of equation 1, imposed on the independent variable, certain of the 32 difference patterns possess the same maximum absolute distance of a point from the least-squares line fit. Identification of identical patterns of differences reduce to eleven the number of essentially different cases. Each of these cases is tabulated below, giving the absolute value of the residual for the farthest point from the least-squares line.

Difference Pattern	Maximum Absolute Residual
1 1 1 1 1	0.0
1 1 1 1 -1	1.4
1 1 1 -1 1	1.4
1 1 1 -1 -1	0.8
1 1 -1 1 1	1.6 greatest maximum residual
1 1 -1 1 -1	1.2
1 1 -1 -1 1	1.2
1 -1 1 1 -1	1.4
1 -1 1 -1 1	1.2
1 -1 -1 1 -1	1.4
1 -1 -1 -1 1	1.2

Since the greatest (absolute) y-distance of one of these points from a least-squares line is 1.6, the theorem, stated in equations 2 and 3, is proved. Note, however, that the theorem provides a sufficient, but not a necessary condition.

With this background, the amplifier module calibration data may be evaluated. The tolerance is adjusted to 0.0078 V (0.0125/1.6). A standard form is used to make difference plots of the calibration data.

If a line can be drawn on the difference plot which passes within 0.0078 V of each data point, the linearity requirement is satisfied. If no such line can be drawn, judgement is deferred, and the part is held for further investigation.

This technique has been successfully applied to reduce delays in a large-scale testing program. About 95% of a large group of amplifier modules which were evaluated using this technique, were accepted without waiting for computer curve fits.

Source: Frances A. Norton Bari of
The Boeing Company
under contract to
Marshall Space Flight Center
(MFS-14834)

No further documentation is available.

GRAPHING THE CUMULATIVE DISTRIBUTION FUNCTION FOR THE PRODUCT FUNCTION

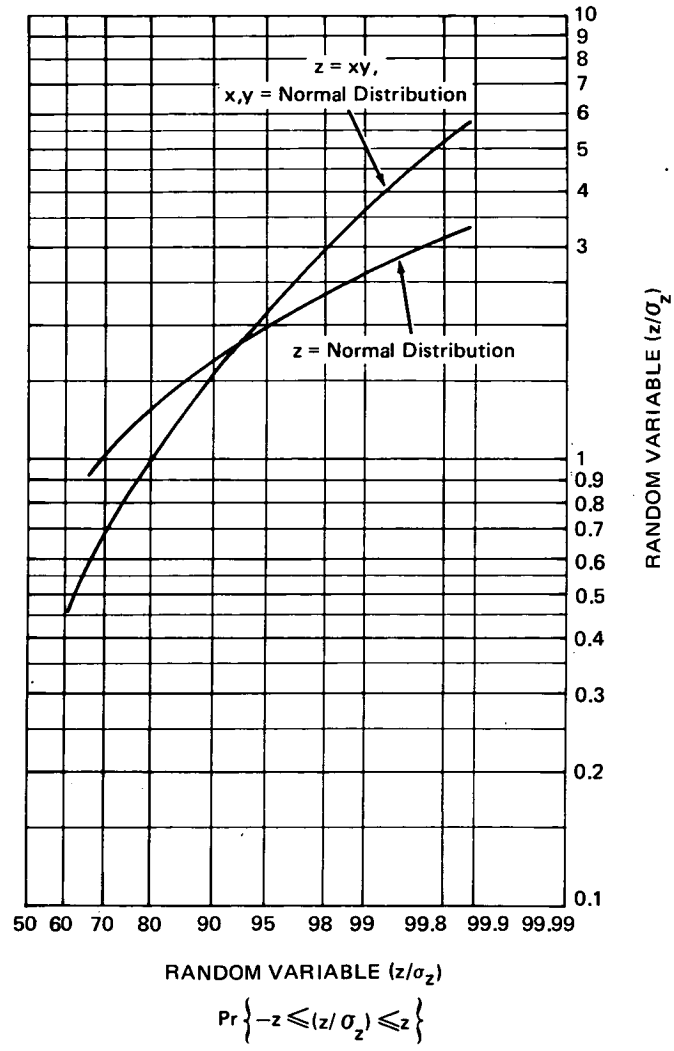

Figure 2. Cumulative Probability Distribution Function for Function of Normal-Distribution Random Variable(s)

A graph has been created that shows the cumulative distribution function (cdf) for the product of two independent normally-distributed random variables, each having zero mean and a unit standard deviation. The graph can be used to find the probability that a positive or a negative deviation of the product variable, as large as or larger than a specified deviation, will occur by chance.

This explicit evaluation for the cdf, previously unrecorded, is now readily available in graphic form (see the figure for an example). It can be helpful in statistical analysis where normal random variables arise.

Source: D. Carden of
Rockwell International Corp.
under contract to
Marshall Space Flight Center
(MFS-16835)

Circle 13 on Reader Service Card.

A LINEAR PROGRAMMING MANUAL

This manual, *Linear Programming Primer,* presents a lucid and useful introduction to linear programming and discusses the use of a computer (the Univac 1108) to solve linear programming problems. The manual can be understood by readers familiar with mathematics at a high school algebra level.

The first part introduces vector spaces and convex sets and presents those elements of matrix algebra used to solve a system of simultaneous linear equations.

The second part introduces the linear programming (LP) problem. Several examples (such as the diet problem, which seeks the most economical way to get a minimum requirement of vitamins A, C, and D from a diet of milk, beef, and eggs) are followed through in stages. The problems are restated in a useful form; the equations and matrices are set up; the solutions are analyzed; and the simplex method is used to obtain the "best" solutions. Restraints, slack variables, and maximized and minimized solutions are also explained in this discussion.

The third and last part of the manual explains how to use a computer to solve the same problems which were discussed in "long-hand" in Part Two. Only the most elementary knowledge of computers is needed to understand the presentation. In this section, the dual problem, reduced cost analysis, ranges, and error analysis are also presented.

The entire manual presents a practical view of linear programming. It avoids excursions into theory and concentrates on providing the background needed to understand and solve most LP problems.

Source: Richard C. Tuey of
Informatics, TISCO, Inc.
under contract to
NASA Headquarters
(HQN-10743)

Circle 14 on Reader Service Card.

AN ALGORITHM FOR FINDING THE GENERALIZED INVERSE OF A MATRIX

A detailed paper reviews the concept of a generalized inverse and introduces a computer algorithm for its determination.

With this algorithm, additional rows or columns are adjoined to the initial matrix. Then the generalized inverse of the composite matrix is determined, as a simple modification of the generalized inverse of the initial matrix.

This technique is of particular value in estimation theory. It can be used with curvefit and estimation procedures when new data or constraints are adjoined on subsequent computational passes. In general, alternate methods only approximate the generalized inverse. Furthermore, this system has a built-in tolerance that allows the use of imperfect computational models.

Source: R. C. Jackson of
TRW Systems Group
under contract to
Johnson Space Center
(MSC-13458)

Circle 15 on Reader Service Card.

EULER COMPUTER

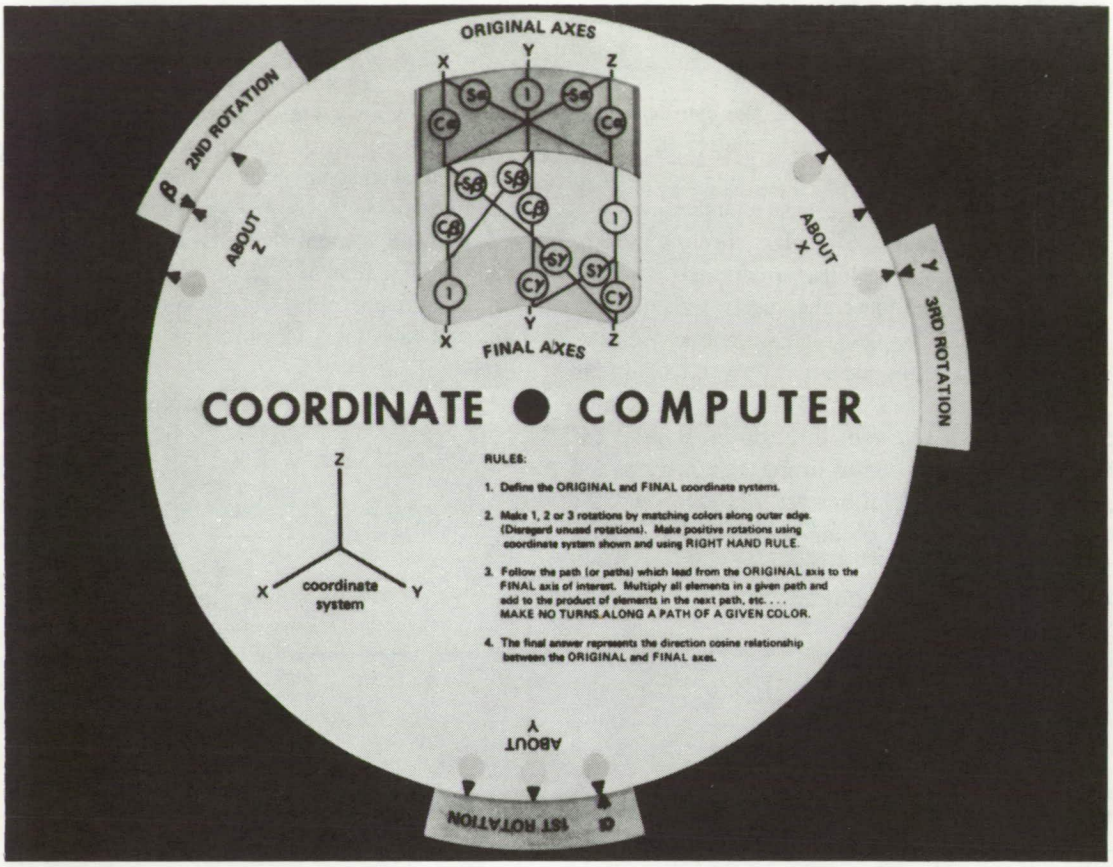

A sophisticated circular slide rule has been developed for computing Euler angles almost instantaneously. Conventional methods, such as unit sphere analysis, require a mathematical background and are time-consuming. In addition, existing calculators have restricted usefulness. The Euler computer has the following advantages:

(a) it provides an unrestricted sequence of three rotations;
(b) it makes the physical relationships clear by diagraming;
(c) it is convenient, fast, accurate, and
(d) can be inexpensively mass produced.

The Euler computer can be used in mechanical design, guidance programing and analysis, stellar navigation, basic-coordinate system mechanization, and for solving complex problems of angular relationships between coordinate systems.

Source: B. W. Robinson of
Rockwell International Corp.
under contract to
Marshall Space Flight Center
(MFS-16868)

Circle 16 on Reader Service Card.

A SLIDE RULE FOR LOGARITHMS

A new circular slide rule has been created. It can be used to rapidly determine logarithmic characteristics (base e or 10). This slide rule has three scales (arabic, $\log_e$, and $\log_{10}$) and a sliding indicator for easy reading. It can be used to convert from one base to another. It is particularly useful for calculating characteristics in the range from 2 through −1, that are required when logarithmic tables are used for multiplication or division.

This slide rule can be used to determine logarithmic characteristics from 0.1 through 100. Circular scales are oriented on two disks, so that an arabic scale on the bottom disk is directly adjacent to the outer scale of the top (inner) rotating disk. These two scales are graduated to be similar to the C and D scales of a conventional slide rule, with the arabic scale identification ranging from 0.1 through 300.

The top (inside) disk also has two separate log scales. One represents $\log_{10}$. It is oriented with the log characteristic "0" in line with the arabic numeral "1" and is graduated through the logarithmic range: −1.0 through 2.4. The second disk represents $\log_e$. It is oriented with the log characteristic "0" in line with the arabic numeral "1" and is graduated through the natural logarithmic range: −2.0 through 5.5. These inner scales are easily read with a rotating indicator, which is assembled, along with the two rotating disks, by a rivet at the origin.

This slide rule could be marketed wherever logarithmic tables are used: in industry, business, and research. It could be mass produced inexpensively by riveting together disks printed by a photographic process.

Source: E. C. Outten, Jr., of
Rockwell International Corp.
under contract to
Marshall Space Flight Center
(MFS-16127)

No further documentation is available.

Section 3. Applied Mathematical Techniques

ACOUSTIC SPECTRAL ANALYSIS AND TESTING TECHNIQUES

Four reports have been published (see references) that outline some recent developments in acoustic spectral analysis. The subjects covered are described below:

The *Octave and One-Third Octave Acoustic Noise Spectrum Analysis* discusses mathematical techniques for combining decibel levels of octaves or constant bandwidths with an overall spectrum level; determining the octave levels in a second octave system when the levels in the first octave are known; and determining the one-third octave levels when the octave levels and the decibels-per-octave slope are known.

In *Power Spectral Density Analysis,* generalized techniques are developed for determining the equation for a power spectral density function. Moreover, an equation is developed that determines the root mean square of a power spectral density function.

The report on *A Digital Technique For Determining 1/3-Octave Sound-Pressure Levels With a More Uniform Confidence Level* describes a computer program that analyzes acoustical test data. The program uses a fast Fourier subroutine to calculate the discrete Fourier coefficients that transform the time-domain data to frequency-domain data. Multiple Fourier transforms are used to convert the narrow-band frequency data to 1/3-octave data.

In the *Acoustic Spectrum Shaping Utilizing Finite Hyperbolic Horn Theory,* sound spectra of high-intensity sound are shaped for single horns and multiple-horn arrays. This technique utilizes computer simulation of horn responses by use of the hyperbolic horn theory.

References:

C. D. Hayes and M. D. Lamers, Technical Report 32-1052, Octave and One-Third Octave Acoustic Noise Spectrum Analysis.

C. D. Hayes, Technical Report 32-928, Revision 1, Power Spectral Density Analysis

J. W. Shipley and R. A. Slusser, Technical Memorandum 33-422, A Digital Technique for Determining 1/3-Octave Sound-Pressure Levels With a More Uniform Confidence Level.

C. D. Hayes, Technical Report 32-1141, Acoustic Spectrum Shaping Utilizing Finite Hyperbolic Horn Theory.

Requests for this documentation and other information may be addressed to:

Technology Utilization Officer
NASA Pasadena Office
4800 Oak Grove Drive
Pasadena, California 91102
Reference: B72-10341

Source: C. D. Hayes, M. D. Lamers,
J. W. Shipley, and R. A. Slusser of
Caltech/JPL
under contract to
NASA Pasadena Office
(NPO-11554)

ANALYTICAL FAILURE DETERMINATION OF FLOW-INDUCED FATIGUE IN BELLOWS

Fatigue failures are experienced in bellows when they carry fluids at high speed. Experience shows that these failures are grouped erratically around Mach 0.3 to Mach 0.4, but the principles governing this behavior are not completely understood. A rigorous treatment of the problem would be very complex and take considerable effort to develop and to follow, but much insight can be obtained by a simple, qualitative analysis.

It can be assumed that flow through a bellows generates sound in the fluid and that the sources of the sound should be repetitive. That is, if the sound is generated by the disturbance in flow past a convolution root, for example, it will be generated at repeating intervals along the bellows corresponding to the convolution spacings. These conditions will amplify certain wavelengths of sound and cancel others, and because the sound travels in both directions, standing waves can be produced. This reasoning applies only to the sound in the fluid and requires no bellows vibration. It would still apply for an infinitely rigid bellows structure. However, the bellows are essentially springs and must be affected to some extent by any varying force such as sound waves. The extent can be expected to range from zero if the natural frequency of the bellows structure opposes and cancels the sound frequency, to a very large magnitude if the natural frequency of the bellows is in phase with and reinforces the sound vibration. The relationship between the sound waves and the spring constants of the bellows can explain the apparently erratic fatigue results.

Using the above assumptions, it is easy to examine the sonic condition in a little more detail. Considering first only a single source of sound (one root), it can be seen that an unknown spectrum of wavelengths will be propagated in all directions with the speed of sound in the fluid. Ignoring all but the axial direction, x, and using a coordinate system fixed to the bellows, it becomes apparent that each wavelength will be greater in the direction of fluid flow than in the opposite direction.

The amplitude of the wave, the sound intensity, will decay in an exponential manner depending on frequency, but if the wave arrives at another source of sound before decay, its residual amplitude will add to the wave from the new source with which it is in phase.

In examining the effects of the sound wave on the bellows structure, the standing wave will tend to cause each root to oscillate back and forth in an opposite direction from each neighboring root. The result will be a flexing of each crest. This mode of vibration explains the metallographic observations in the referenced report which notes that the crests were heavily cold worked in service, while the roots were undisturbed. The natural frequency of the bellows in this type of vibrating notion is therefore critical.

The above analysis was derived rather easily and appears to be qualitatively correct. Greater effort would be required to derive a quantitative expression which would show rate of sound amplification. It is suggested that this analysis be continued to derive such a quantitative description, because one obvious design device to allow high flow rates would be to introduce a half wavelength interruption in the convolutions just prior to the number of convolutions at which the intensity would reach a dangerous level. This would cause destructive interference between the two standing waves and eliminate the vibrations.

Source: R. G. Cron of
Rocketdyne, a Division of
North American Rockwell Corp.
under contract to
Marshall Space Flight Center
(MFS-18178)

Circle 17 on Reader Service Card.

EQUATIONS TO ASSESS THE IMPACT RESISTANCE OF FIBER COMPOSITES

Impact resistance is an important aspect in the design of components made from fiber composite structural materials. Although some basic work on the impact resistance of these materials had been reported, the understanding of impact resistance of fiber composites had not advanced sufficiently for structural components to be designed with predictable impact resistance. Recently, however, equations to assess the impact resistance of fiber composites and convenient design procedures have been developed which are a significant step in this direction. The following two such equations were derived using composite micromechanics and structural mechanics concepts. Equation (1), for longitudinal impact resistance, applies to screening fibers used in composites for impact applications. Equation (2) corresponds to a design concept, referred to as the "hybrid composite concept." It is shown below applied to a cantilever to illustrate the various mechanisms available in this design concept to absorb impact energy. Both equations are applicable to unidirectional composites.

Longitudinal Impact Resistance

The longitudinal impact resistance is often expressed as the impact energy density (IED). IED values of composites with a ratio of fiber modulus to matrix modulus (E_f/E_m) greater than twenty is given by:

$$\text{IED} = \frac{(1 - k_v)\, k_f\, \beta_{fT}^2\, S_{fT}^2}{2E_f} \qquad (1)$$

with an approximation error of less than five percent. In this equation, k_v and k_f denote void and fiber volume ratios, respectively; β_{fT} is the translation coefficient or ratio of fiber tensile strengths in and out of the composite and is taken as unity if not known; S_{fT} is the fiber tensile strength out of the composite (f denotes fiber and T denotes "under tension"); and E_f is the longitudinal fiber modulus.

Potential impact resistance of various fiber composites as predicted by this equation are plotted in the figure as a function of S_{fT}/E_f. Corresponding rankings of fiber composites with 50% fiber to volume ratio normalized with respect to a boron/epoxy composite are listed in the table.

RELATIVE IMPACT RESISTANCE OF VARIOUS AVAILABLE FIBER COMPOSITES

Composite	Rank Relative to Boron/Epoxy Composite
Modmor-I/Epoxy	.30
Thornel-50S/Epoxy	.33
Thornel-75/Epoxy	.53
Boron/Epoxy	1.00
Modmor-II/Epoxy	1.04
Thornel-400/Epoxy	1.68
PRD-49/Epoxy	1.82
E-Glass/Epoxy	3.70
UARL-344-Glass/Epoxy	8.00
S-Glass/Epoxy	10.20

In the equation (1), IED is not directly dependent on the resin properties. However, some influence of the resin properties enters the equation through β_{fT}.

Hybrid Composite Concept

Hybrid composites are usually made by laminating together plies or laminates from two different fiber/matrix systems. The equation utilizing the hybrid composite concept to design a cantilever, whose core and faces (shell) are made from two different fiber/matrix systems, is given by:

$$\text{IED} = \frac{1}{2}\frac{S^s_{l11T}}{E^s_{l11}}\left\{\left[\frac{1}{9} + \frac{1}{30}\left(\frac{h}{l}\right)^2 \left(\frac{E^a_{l11}}{G^a_{l12}}\right)\right] + \frac{1}{16N_{LD}}\left(\frac{h}{l}\right)\frac{E^s_{l11}}{S^c_{l12}} + \frac{\pi}{16}\left(\frac{N_{fD}d_f^3}{bhl}\right)\left(\frac{E^s_{l11}}{S^s_{l12}}\right)\left(\frac{S^s_{fT}}{S^s_{l11T}}\right)^2\right\} \qquad (2)$$

where the superscripts (a), (s), and (c) represent averaged core-shell, shell, and core, respectively. The subscript (l) refers to unidirectional composite properties along

the direction indicated by the numerical subscripts following (l). The variables b, h, and (l) represent width, depth, and length of the cantilever, respectively. The variables d_f, N_{fD} and N_{LD} represent fiber diameter, number of fibers that pulled out, and number of layers that delaminated, respectively. The variables E, S, and G denote normal modulus (compression or tension), strength, and shear modulus of the composite, respectively.

Examining this equation reveals that the shear contribution depends on E^a_{l11}/G^a_{l12}, and both fiber pull-out and delamination depend on the parameter E_{l11}/S_{l12}. This means that in order to take advantage of the high shear contribution of fiber pull-out and/or delamination, high longitudinal modulus, low shear modulus, and low intralaminar shear strength composites should be selected.

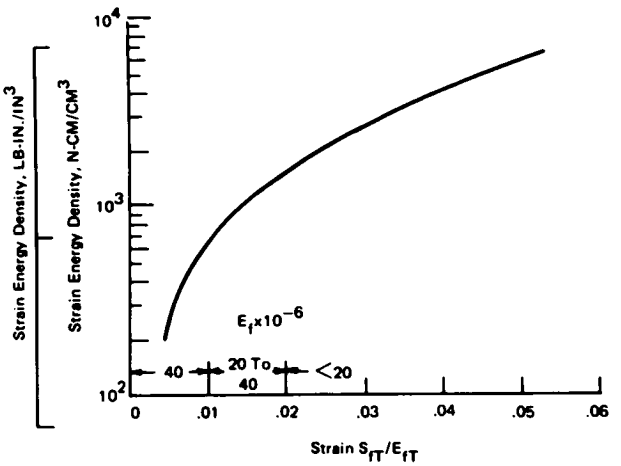

Potential Impact Resistance Of Fiber Composite Materials From The Table

Most commercial composites containing various types of fibers in a resin matrix meet this criterion.

These equations have several possible applications. They can be used in the design of any composite structural component subjected to impact; for example, compressor blades, pipes, wall or roof panels, and many others. The longitudinal impact resistance equation can be used by designers, researchers, and fabricators of fiber composite components in selecting fibers for impact applications. Furthermore, the hybrid composite concept can be used by designers in numerous industries such as aircraft, aerospace, marine, construction, and other commercial industries.

The following documentation may be obtained from:

National Technical Information Service
Springfield, Virginia 22151
Single document price $3.00
(or microfiche $2.25)

Reference: NASA TM-X-67802 (N71-24010), Impact Resistance of Unidirectional Fiber Composites

Reference: NASA TN-D-6463 (N71-32243), Designing for Impact Resistance with Unidirectional Fiber Composites

Source: Christos C. Chamis, Morgan P. Hanson, and Tito T. Serafini
Lewis Research Center
(LEW-11486)

LOAD-RELIEF CONTROLLER EMPLOYS STOCHASTIC MINIMIZATION TECHNIQUE

A mathematical study of the control of a launch booster, disturbed by winds, offers general techniques that may be useful in other statistical and optimization problems.

In launching missiles, winds cause bending, rotations, and translations of the launch booster. The booster is controlled by gimbaling part of its thrust. A gimbal controller is designed to allow gimbal motions to compensate for the undesired wind effects.

The load-relief problem is formulated as a stochastic minimization problem. The incident winds and corresponding booster responses are treated as random processes, and an event of mission failure is defined. The stochastic problem is to minimize an upper bound on the likelihood of occurrence of this event.

Based on this analysis, several controllers were designed for a study vehicle. Digital and analog simulations showed that these controllers provided excellent load relief. They were not parameter sensitive, they could be successfully simplified, and they generally were superior to controllers designed by frozen-point methods.

Source: G. B. Skelton of
Honeywell, Inc.
under contract to
Marshall Space Flight Center
(MFS-91764)

Circle 18 on Reader Service Card.

EXTRAPOLATING WIND-SHEAR INFORMATION FOR LOW ALTITUDES FROM THAT FOR HIGH ALTITUDES

Statistical wind-shear information has been used to construct synthetic wind profiles for the design of space vehicles. Because some space-vehicle sites lack detailed wind-profile data for altitudes less than 1 km, a new method was developed to extrapolate wind-shear information for these altitudes from the more-available data on altitudes greater than 1 km. Mathematical analysis is used to generate probability distribution functions and other related information for the wind shear.

It is assumed that any scalar wind profile, from an ensemble of wind profiles, can be represented by terms of a Fourier integral. The integrals permit the ensemble variance and the mean of the wind shears to be related to the power spectrum of the wind-profile ensemble.

Meteorologists and the designers and operators of aircraft who need to know the behavior of winds aloft will find this method of interest.

Source: George H. Fichtl of
Marshall Space Flight Center
(MFS-21181)

Circle 19 on Reader Service Card.

TURBULENT MIXING FILM COOLING CORRELATION

A film cooling effectiveness correlation has been developed to predict the film cooling air flow requirements for gas turbine combustors. Film cooling experiments were conducted in a rectangular sector of a high performance gas turbine combustor where the hot stream turbulence was high. Cooling air was injected through various slot configurations, and film cooling effectiveness was determined by wall temperature measurements on the combustor liner downstream of the slots.

The data from the experiments were compared to several correlations in the literature, and the agreement between the predicted and the experimental values was poor. Some of the literature correlations overestimated the film cooling effectiveness by a factor of five or more.

A turbulent mixing model was developed to account for the high mixing rate which occurs between the cooling film and the hot gas stream in the combustor. The mixing rate in combustors is much higher than that occurring under low turbulence conditions for which correlations have been developed. The resulting equation correlated the data to within ± 20 percent. The new correlation is given by:

$$\eta = \frac{1}{1 + C_m \frac{x}{MS}} \qquad (1)$$

where

$$\eta = \text{film cooling effectiveness} = \frac{T_h - T_w}{T_h - T_c}$$

x = downstream distance from slot exit
S = slot height
M = mass flux ratio of the film to the hot gas (film mass flow rate/slot flow area)/(hot gas flow rate/combustor flow area)

C_m = mixing coefficient
T_h = temperature of the hot gas
T_w = wall temperature
T_c = coolant inlet temperature

The mixing coefficient, C_m, is a measure of the intensity and scale of turbulence and equalled 0.15 for the combustor used. This value was determined by comparing equation (1) with experimental film cooling data, and it was also verified by hot wire measurements within the combustor during cold flow tests.

The correlation also predicted data in the literature taken in low turbulence wind tunnels with typical turbulence levels of approximately one percent; a value of 0.01 for C_m correlated these data.

The new correlation has the following advantages:

1. It can correlate data from widely different flow regimes if the turbulent mixing level can be measured or estimated.
2. The variation of film cooling effectiveness with turbulence level can readily be estimated from the correlation.
3. It is simple to apply, the only input value necessary being: effective slot height, s; mass flux ratio, M; downstream distance, x; and turbulent mixing level, C_m.

The following documentation may be obtained from:

National Technical Information Service
Springfield, Virginia 22151
Single document price $3.00
(or microfiche $2.25)

Reference: NASA TN-D-6360, (N71-29841), Combustor Liner Film Cooling in Presence of High Free-Stream Turbulence

Source: Albert J. Juhasz and
Cecil J. Marek
Lewis Research Center
(LEW-11417)

IMPROVEMENTS OF ZEYDEL METHOD FOR CALCULATING FLUTTER OF FLAT PANELS

A report has been published which discusses Zeydel's exact method for calculating flutter boundaries and estimating stresses in an infinite spanwise array of panels. The theory is based on the exact linearized inviscid aerodynamic theory. A general analysis of orthotropic panels is presented that accounts for different edge conditions, elastic foundation, membrane stresses, and viscous and structural damping. Various results are presented for very long panels. Two limits of the exact theory are discussed that correspond to the simple static aerodynamic theory approximation and the traveling-wave theory, respectively. A further result for the mode shape of a semi-infinite panel is presented that shows how a traveling wave is amplified and reflected by the trailing edge.

Extensive numerical calculations are presented for the special case of pinned edge panels, isotropic panel material, zero viscous damping, and no elastic foundation. Comparisons are made with previous results that verify the computational procedure. Design flutter boundaries of mass ratio versus length-to-width ratio are presented for different materials and altitude. Typical mode shapes are also given. The effect of structural damping at different Mach numbers and length-to-width ratios is discussed. Example calculations of the stress level in a panel are made.

Design flutter boundaries are presented for aluminum panels on a typical Saturn V trajectory. Flutter is indicated for certain panels on the forward skirt of the S-IVB stage, that is in agreement with in-flight data. Because of the relatively short duration of flutter, it is concluded that failure is not likely to occur.

Source: J. E. Yates of
Aeronautical Research Associates of Princeton, Inc.
under contract to
Marshall Space Flight Center
(MFS-20955)

Circle 20 on Reader Service Card.

Patent Information

The following innovation, described in this Compilation, has been patented or is being considered for patent action as indicated below:

Binary Concatenated Coding System (Page 2) MSC-14082

This invention is owned by NASA, and a patent application has been filed. Inquiries concerning nonexclusive or exclusive license for its commercial development should be addressed to:

Patent Counsel
Johnson Space Center
Code AM
Houston, Texas 77058

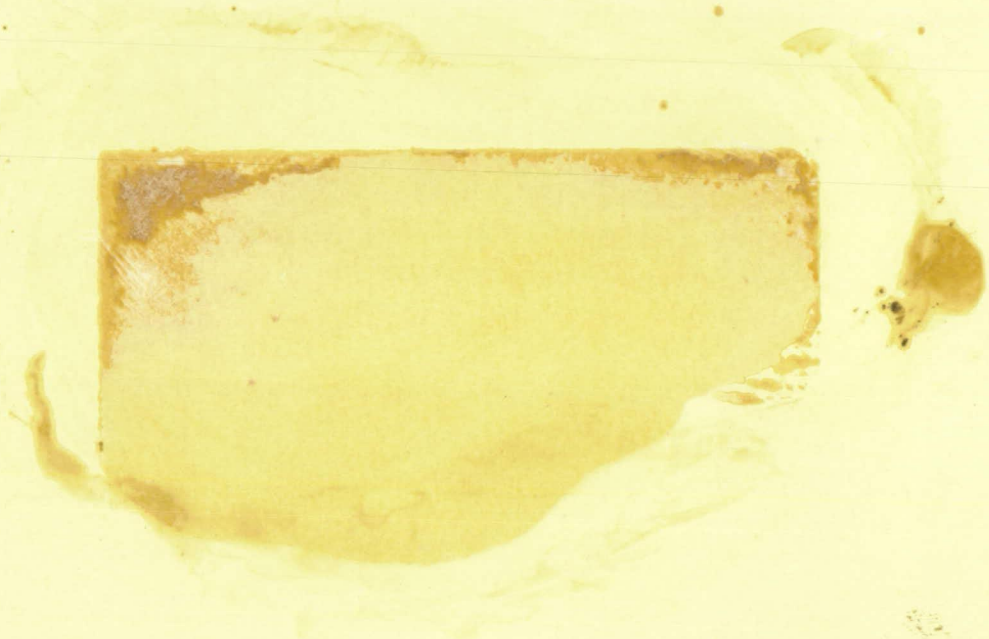

"The aeronautical and space activities of the United States shall be conducted so as to contribute . . . to the expansion of human knowledge of phenomena in the atmosphere and space. The Administration shall provide for the widest practicable and appropriate dissemination of information concerning its activities and the results thereof."

—NATIONAL AERONAUTICS AND SPACE ACT OF 1958

NASA TECHNOLOGY UTILIZATION PUBLICATIONS

These describe science or technology derived from NASA's activities that may be of particular interest in commercial and other non-aerospace applications. Publications include:

TECH BRIEFS: Single-page descriptions of individual innovations, devices, methods, or concepts.

TECHNOLOGY SURVEYS: Selected surveys of NASA contributions to entire areas of technology.

OTHER TU PUBLICATIONS: These include handbooks, reports, conference proceedings, special studies, and selected bibliographies.

Details on the availability of these publications may be obtained from:

National Aeronautics and
Space Administration
Code KT
Washington, D.C. 20546

Technology Utilization publications are part of NASA's formal series of scientific and technical publications. Others include Technical Reports, Technical Notes, Technical Memorandums, Contractor Reports, Technical Translations, and Special Publications.

Details on their availability may be obtained from:

National Aeronautics and
Space Administration
Code KS
Washington, D.C. 20546

NATIONAL AERONAUTICS AND SPACE ADMINISTRATION
Washington, D.C. 20546